Analysis of ESCRT functions in exosome biogenesis, composition and secretion highlights the heterogeneity of extracellular vesicles

Marina Colombo[1,2,3], Catarina Moita[4], Guillaume van Niel[1,3], Joanna Kowal[1,2], James Vigneron[1,2], Philippe Benaroch[1,2], Nicolas Manel[1,2], Luis F. Moita[4], Clotilde Théry[1,2,*,‡] and Graça Raposo[1,3,*,‡]

[1]Institut Curie Section Recherche, 26 rue d'Ulm, 75248 Paris cedex 05, France
[2]INSERM U932, 26 rue d'Ulm, 75248 Paris cedex 05, France
[3]CNRS UMR144, 26 rue d'Ulm, 75248 Paris cedex 05, France
[4]Instituto de Medicina Molecular, Faculdade de Medicina, Universidade de Lisboa, 1649-028 Lisboa, Portugal

*These authors contributed equally to this work
‡Authors for correspondence (clotilde.thery@curie.fr; graca.raposo@curie.fr)

Accepted 20 September 2013
Journal of Cell Science 126, 5553–5565

doi: 10.1242/jcs.128868

Summary

Exosomes are extracellular vesicles (EVs) secreted upon fusion of endosomal multivesicular bodies (MVBs) with the plasma membrane. The mechanisms involved in their biogenesis have not yet been fully identified although they could be used to modulate exosome formation and therefore are a promising tool in understanding exosome functions. We have performed an RNA interference screen targeting 23 components of the endosomal sorting complex required for transport (ESCRT) machinery and associated proteins in MHC class II (MHC II)-expressing HeLa-CIITA cells. Silencing of *HRS*, *STAM1* or *TSG101* reduced the secretion of EV-associated CD63 and MHC II but each gene altered differently the size and/or protein composition of secreted EVs, as quantified by immuno-electron microscopy. By contrast, depletion of VPS4B augmented this secretion while not altering the features of EVs. For several other ESCRT subunits, it was not possible to draw any conclusions about their involvement in exosome biogenesis from the screen. Interestingly, silencing of *ALIX* increased MHC II exosomal secretion, as a result of an overall increase in intracellular MHC II protein and mRNA levels. In human dendritic cells (DCs), ALIX depletion also increased MHC II in the cells, but not in the released CD63-positive EVs. Such differences could be attributed to a greater heterogeneity in size, and higher MHC II and lower CD63 levels in vesicles recovered from DCs as compared with HeLa-CIITA. The results reveal a role for selected ESCRT components and accessory proteins in exosome secretion and composition by HeLa-CIITA. They also highlight biogenetic differences in vesicles secreted by a tumour cell line and primary DCs.

Key words: Extracellular vesicles, Exosomes, ESCRT, MHC class II, ALIX

Introduction

Although there is still some debate about the exact definition (Gould and Raposo, 2013), exosomes are generally defined as secreted extracellular vesicles (EVs) corresponding to the intralumenal vesicles (ILVs) of multivesicular bodies (MVBs), which are formed during the maturation of these endosomes. Some MVBs are fated for degradation, whereas others can fuse with the plasma membrane, leading to the secretion of ILVs as exosomes (Bobrie et al., 2011; Raposo and Stoorvogel, 2013). The generation of the ILVs into MVBs involves the lateral segregation of cargo at the endosomal limiting membrane, the formation of an inward budding vesicle and the release in the endosomal lumen of the membrane vesicle containing a small portion of cytosol. Over the past 10 years several studies have started to elucidate the mechanisms involved in ILV formation and cargo sorting (Hanson and Cashikar, 2012; Henne et al., 2011; Hurley, 2008; Raiborg and Stenmark, 2009). Given that exosomes correspond to ILVs, the same mechanisms are thought to be involved in their biogenesis. However, cells contain different populations of MVBs and ILVs (Buschow et al., 2009; Möbius et al., 2003; White et al., 2006) and we are still at an early stage of understanding the mechanisms that contribute to exosome formation and cargo sorting within these vesicles.

The components of the endosomal sorting complex required for transport (ESCRT) are involved in MVB and ILV biogenesis. ESCRTs consist of approximately twenty proteins that assemble into four complexes (ESCRT-0, -I, -II and -III) with associated proteins (VPS4, VTA1, ALIX), which are conserved from yeast to mammals (Henne et al., 2011; Roxrud et al., 2010). The ESCRT-0 complex recognizes and sequesters ubiquitylated proteins in the endosomal membrane, whereas the ESCRT-I and -II complexes appear to be responsible for membrane deformation into buds with sequestered cargo, and ESCRT-III components subsequently drive vesicle scission (Hurley and Hanson, 2010; Wollert et al., 2009). ESCRT-0 comprises HRS that recognizes the mono-ubiquitylated cargo proteins and associates in a complex with STAM, Eps15 and clathrin. HRS recruits TSG101 of the ESCRT-I complex, and ESCRT-I is then involved in the recruitment of ESCRT-III, through ESCRT-II or ALIX, an ESCRT-accessory protein. Finally, the dissociation and

recycling of the ESCRT machinery requires interaction with the AAA-ATPase Vps4. It is unclear whether ESCRT-II has a direct role in ILV biogenesis or whether its function is limited to a particular cargo (Bowers et al., 2006; Malerød et al., 2007).

Concomitant depletion of ESCRT subunits belonging to the four ESCRT complexes does not totally impair the formation of MVBs, indicating that other mechanisms may operate in the formation of ILVs and thereby of exosomes (Stuffers et al., 2009). One of these pathways requires a type II sphingomyelinase that hydrolyses sphingomyelin to ceramide (Trajkovic et al., 2008). Although the depletion of different ESCRT components does not lead to a clear reduction in the formation of MVBs and in the secretion of proteolipid protein (PLP) associated to exosomes, silencing of neutral sphingomyelinase expression with siRNA or its activity with the drug GW4869 decreases exosome formation and release. However, whether such dependence on ceramides is generalizable to other cell types producing exosomes and additional cargos has yet to be determined. The depletion of type II sphingomyelinase in melanoma cells does not impair MVB biogenesis (van Niel et al., 2011) or exosome secretion (our unpublished data) but in these cells the tetraspanin CD63 is required for an ESCRT-independent sorting of the luminal domain of the melanosomal protein PMEL (van Niel et al., 2011). Moreover, tetraspanin-enriched domains have been recently proposed to function as sorting machineries allowing exosome formation (Perez-Hernandez et al., 2013).

Despite evidence for ESCRT-independent mechanisms of exosome formation, proteomic analyses of purified exosomes from various cell types have identified ESCRT components (TSG101, ALIX) and ubiquitylated proteins (Buschow et al., 2005; Théry et al., 2001). It has also been reported that the ESCRT-0 component HRS could be required for exosome formation and/or secretion by dendritic cells (DCs), and thereby impact on their antigen-presenting capacity (Tamai et al., 2010). The transferrin receptor (TfR) in reticulocytes that is generally fated for exosome secretion, although not ubiquitylated, interacts with ALIX for MVB sorting (Géminard et al., 2004). More recently it was also shown that ALIX is involved in exosome biogenesis and exosomal sorting of syndecans through its interaction with syntenin (Baietti et al., 2012).

Nonetheless, as discussed above and elsewhere (Bobrie et al., 2011) and because in most studies only one or few selected ESCRT subunits and accessory proteins have been analysed, it is still unclear whether ESCRT components are involved at any step in the formation of exosomes. Here, we have used RNA interference (RNAi) to target 23 different components of the ESCRT machinery and associated proteins in major histocompatibility complex class II (MHC II)-expressing HeLa cells. To specifically analyse the effect of these ESCRT components on secretion of MVB-derived vesicles (i.e. exosomes), we characterized and quantified the released vesicles for the endosomal tetraspanin CD63, MHC II and either the endosome-associated heat shock protein HSC70 or the tetraspanin CD81. Our results demonstrate a role for a few selected members of this family in either the efficiency of secretion or the size and composition of the secreted vesicles. In addition, they highlight differences in exosomes secreted by these cells and primary MHC-II-expressing DCs, in terms of size and content of some exosomal proteins.

Results

Selected ESCRT proteins modulate exosome biogenesis or secretion

In order to determine whether different ESCRT components affect exosome biogenesis or secretion, we performed a small hairpin RNA (shRNA)-based screen targeting twenty-three ESCRT proteins in a 96-well plate format as previously set up in our group (Ostrowski et al., 2010). HeLa-CIITA-OVA cells were used as a model cell line because they express MHC II molecules which allow us to monitor exosome secretion, and they secrete ovalbumin (OVA) which is useful to assess the classical secretion pathway. These cells were infected with lentiviral vectors encoding shRNA sequences specific for individual ESCRT proteins: five different shRNA sequences were used to knock down each gene, and the control was an shRNA that does not target any human sequences (shSCR). shRNA-expressing cells selected by puromycin were incubated for 48 hours with exosome-depleted medium. Secreted exosomes were then trapped on anti-CD63-coated beads [because CD63 accumulates on ILVs of MVBs in HeLa-CIITA (Ostrowski et al., 2010)] and detected by flow cytometry with anti-CD81 and anti-HLA-DR (MHC II) antibodies, two molecules commonly detected in most EVs (Escola et al., 1998; Zitvogel et al., 1998). To monitor the classical secretory pathway of soluble proteins, ovalbumin was similarly trapped on anti-OVA beads and detected with an anti-OVA antibody (Fig. 1A). Finally, the efficiency of the silencing of each gene was analysed in exosome-secreting cells by quantitative RT-PCR (qRT-PCR). The criterion used to identify a gene as potentially involved in exosome secretion was that at least two different shRNA sequences, which inhibited gene expression either significantly or by at least 50%, would modulate exosome secretion in the same manner. Only shRNA that did not affect cell proliferation or survival were considered for further analysis.

The results of the screen are summarized in Table 1: among the 23 candidates analysed, seven were not further analysed for effects on exosome secretion because of the inability to demonstrate a downregulation of the gene. shRNA specific for four of the candidates did not induce a significant modulation of exosome secretion (supplementary material Fig. S1), and five of them showed inconsistent effects of the different shRNA sequences on exosome secretion (supplementary material Fig. S2). Therefore, we are not able to draw any conclusions on the involvement of these 16 genes in exosome secretion.

The remaining seven candidates met the defined selection criterion; a second round of screening then confirmed selected hits. As shown in Fig. 1B, inhibiting three ESCRT-0/I proteins (HRS, STAM1 and TSG101) induced a decrease in exosome secretion: two or more different shRNA sequences (sh1 and sh3 for *HRS*, sh2 and sh3 for *STAM1*, all shRNA for *TSG101*) induced at least 50% inhibition in exosome secretion. Conversely, inhibition of four ESCRT-III disassembly and accessory proteins (CHMP4C, VPS4B, VTA1, ALIX) induced an increase in exosome secretion (Fig. 1C): at least two shRNA sequences (sh3 and sh5 for *CHMP4C* and *VPS4B*, sh1 and sh3 for *VTA1* and *ALIX*) induced an increase of 50% or more in exosome secretion as measured by our FACS-based assay. Both sh1 and sh3 targeting *ALIX*, were selected as candidate sequences because they both lead to a similar phenotype of increased secretion of exosomes, despite sh4 decreasing the level of *ALIX* expression more than the other sequences. Secretion of OVA was not affected

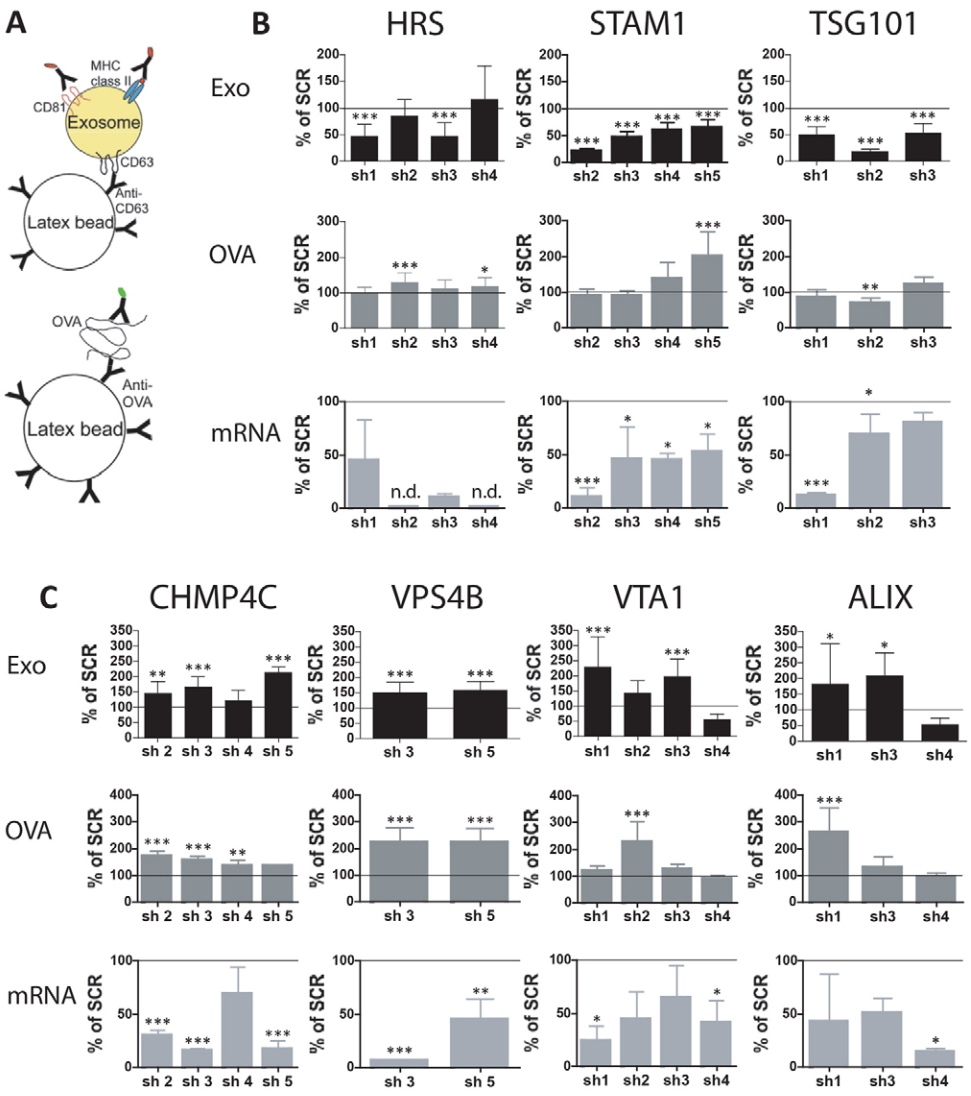

Fig. 1. Modulation of exosome secretion by members of the ESCRT family as evidenced by the screening of a library of shRNA. (A) Exosomes and ovalbumin (OVA) in cell-conditioned medium were measured by trapping each on a separate antibody-coated bead, staining the beads with exosome- or OVA-specific antibodies coupled to different fluorophores, and analysing the beads by flow cytometry. (B,C) Exosome secretion (top row), ovalbumin secretion (middle row) and gene downregulation (bottom row) are shown for genes whose silencing induced a decrease in exosome secretion (B), or an increase in exosome secretion (C). Results are shown as percentage of the control (shSCR) measured as arbitrary units (AU); values are means ± s.d. of three experiments performed in triplicate. The black horizontal line indicates the level of the control (shSCR, 100%), n.d., not determined. One-way ANOVA followed by Tukey's post test, $*P<0.05$, $**P<0.01$, $***P<0.001$.

by most shRNA sequences allowing depletion of HRS, STAM1, TSG101, VTA1 and ALIX. Silencing of *CHMP4C* and *VPS4B* induced a significant ($P<0.001$) increase (over 100% in the case of *VPS4B*, and between 50 and 80% for *CHMP4C*) in secreted OVA with most shRNA sequences. These data suggest that these components may also have an impact on the classical secretion pathway of proteins.

Validation of the screen results by western blot analysis of secreted exosomes

We then chose one shRNA to validate the results of the screen, by analysing exosomes produced by large numbers of cells ($1–2\times10^8$ cells), using classical purification procedures (Théry et al., 2006). Of the two shRNAs that modulated exosome secretion in the same manner (listed in the previous section), we selected the one that induced the largest mRNA decrease (sh3 for *HRS*, *CHMP4C* and *VPS4B*, sh2 for *STAM1*, sh1 for *TSG101*, *VTA1* and *ALIX*). Exosomes were purified by differential ultracentrifugation of the supernatant of shRNA-expressing HeLa-CIITA-OVA cells as previously described (Théry et al., 2006), and the pellet obtained in the final 100,000 ***g*** ultracentrifugation was analysed by western blotting for the presence of MHC II, CD63 and a chaperone described previously as enriched in exosomes secreted by mouse DCs, HSC70 (Théry et al., 1999) (Fig. 2A–D; supplementary material Fig. S3). Three experiments were performed, in which we also assessed the efficient downregulation of each target gene by qRT-PCR or western blotting of total cell lysates (supplementary material Fig. S4).

Secretion of all markers was decreased, compared with control cells, in HRS-, STAM1- and TSG101-depleted cells, which suggests a decrease in total exosome secretion by these cells. In the case of CHMP4C and VTA1 depletion, we observed no change, or even a slight decrease, in the signal of all three markers, which does not confirm the initial conclusion from the screen, where we detected an increase in exosome secretion (Fig. 1C). *VPS4B* silencing induced an increase in all markers, as compared with exosomes from shSCR-treated cells, which indicates an increase in total secretion of exosomes, in agreement with the results from the screen. Interestingly, the silencing of *ALIX* caused a clear increase in MHC II in the three experiments, but produced more variable effects on the levels of HSC70 and CD63 as compared with control exosomes. These results suggest a change in exosome composition due to ALIX depletion, rather than a change in exosome yield.

To confirm the effects of gene silencing observed with one shRNA, a similar western blot analysis of exosomes secreted in a large-scale set up was performed using the other shRNA that had a similar effect in the screen (Fig. 1). This further confirmed that inhibiting these genes by two different shRNA sequences either decreased (*HRS*, *STAM1*, *TSG101*) or increased (*VPS4B*) overall exosome secretion (Fig. 2E).

Immuno-electron microscopy analysis of exosomes released by ESCRT-depleted cells

To investigate the morphology and CD63 and MHC II content of the vesicles secreted by shRNA-treated cells compared with control cells, we characterized exosomes by immuno-electron microscopy (IEM) in a quantitative manner: 100,000 ***g*** pellets were analysed as whole-mount samples immunogold-labelled for MHC II and CD63 (Fig. 3A). The diameter and the number of gold particles corresponding to each marker were evaluated independently two to four times per condition in 200 vesicles per condition. First, we observed that the proportion of vesicles of different sizes was modified upon silencing of some ESCRT components (Fig. 3B). The majority of vesicles from shSCR-, shVPS4B- or shTSG101-treated cells had a diameter of 50–100 nm (Fig. 3B, upper panel). By contrast, shHRS treatment slightly increased the proportion of smaller vesicles (below 50 nm; Fig. 3B, middle panel), whereas silencing of *STAM1* or *ALIX* increased the proportion of larger vesicles (above 100 nm, Fig. 3B, lower panel).

By quantifying the presence of CD63 and MHC II in vesicles of different sizes, we observed that CD63 was most enriched on smaller vesicles, whereas MHC II was detected more prominently on larger vesicles, and less than 20% of the total vesicles had both proteins (Fig. 3C). It should be noted, however, that absence of labelling does not imply that these proteins are completely absent, only that their level is too low to be detected. These observations indicate that, in addition to vesicles with a classical size of exosomes analysed as whole-mount by EM (50–100 nm), at least two other different types of vesicles are present in the 100,000 ***g*** pellet: smaller vesicles (30–50 nm) enriched in CD63, and vesicles with a larger diameter (100–200 nm) and a higher MHC II content. In addition, in some cases manipulation of ESCRT expression induced differences in the protein content of the secreted vesicles. The depletion of VPS4B or HRS (Fig. 3C) did not strikingly alter the CD63 and MHC II content of the different types of vesicles. By contrast, depletion of TSG101 and STAM1 caused an increase in the proportion of vesicles of all sizes devoid of CD63 and MHC II (Fig. 3C,D). Conversely, depletion of ALIX induced a substantial increase in the proportion of vesicles labelled with MHC II, alone or together with CD63, among all categories defined by size (Fig. 3C,D). This observation is in agreement with the above result from western blotting of an increase in MHC II content in shALIX-derived exosomes.

We have so far observed an important heterogeneity of the vesicles purified by the differential ultracentrifugation procedure classically used for exosome purification, not only in terms of size but also of protein content. Interestingly, depletion of HRS and STAM1 induced a general decrease in secretion of vesicle-associated CD63 and MHC II (as observed by western blotting; Fig. 2). With the former, however, the vesicles were also smaller, whereas with the latter they were larger than control vesicles. The most remarkable effect was observed upon depletion of ALIX, which induced the secretion of an increased proportion of larger vesicles, and an altogether higher MHC II content.

ALIX-depleted HeLa cells have a higher MHC II content

In order to understand the effect induced by shALIX on exosomes secreted by HeLa-CIITA-OVA cells, we analysed total cell lysates by western blotting (Fig. 4A): we confirmed the decrease of ALIX in shRNA-expressing cells, and we quantified an increase in MHC II content in these cells (between 25 and 140%), as compared with reference proteins (HSC70 or actin depending on the experiment). The increase in MHC II in ALIX-depleted cells was also observed at the cell surface, as shown by fluorescence-activated cell scanning (FACS) of non-permeabilised cells (Fig. 4B), but the levels of CD63 were on average not significantly modified compared with control cells. Finally, quantitative IEM analysis of ultrathin cryosections labelled for MHC II and CD63 (Fig. 4C) showed that MHC II was higher, whereas CD63 was unaltered in the MVBs of cells depleted of ALIX, compared with control cells. Therefore we

Table 1. Summary of the screening results

Most shRNAs modulate exosome secretion	Most shRNAs have no effect on exosome secretion	Divergent effects of the different shRNAs in terms of exosome secretion	Gene not silenced/not expressed/qPCR not interpretable
ESCRT-0			
HRS/HGS	VPS28	STAM2	
STAM1/STAM			
ESCRT-I			
TSG101	VPS37A		VPS37B
ESCRT-II			
	SNF8	VPS36	
	VPS25		
ESCRT-III			
CHMP4C		CHMP1B	CHMP2A
		CHMP5	CHMP2B
		CHMP6	CHMP4A
			CHMP4B
			CHMP3
Disassembly complex/Accessory proteins			
VPS4B			VPS4A
VTA1			
ALIX/PDCD6IP			

The common name (used throughout the text) is indicated together with the official symbol when different.

observed a general increase of MHC II in cells upon *ALIX* knockdown, both at the cell surface and in intracellular MVBs.

This overexpression could be due to an increased transcription of the MHC II genes, translation of the mRNA, or stability of the protein (i.e. less degradation). To test the first hypothesis, we performed reverse transcription followed by qRT-PCR on mRNA extracted from shSCR- or shALIX-treated cells. As shown in Fig. 5A, upon *ALIX* silencing we observed an increase of at least 50% and generally more than 200% in the expression of MHC II beta (HLA-DRB1) and alpha (HLA-DRA) chains, whereas CD63 mRNA was modulated in a variable manner, showing a slight increase in only half of the experiments. We then re-expressed ALIX in shALIX-expressing cells, using a cDNA with silent mutations in the shRNA-binding site, and observed a decrease in the HLA-DR mRNA level, although not at the same levels as in the shSCR control cells, which can be expected for a rescue experiment (Fig. 5B). These results indicate that ALIX modulates HLA-DR expression at the mRNA level, showing an unexpected effect of ALIX on mRNA expression or stability.

Silencing of *ALIX* results in an increase in MHC II content in human immature DCs

We next investigated whether the increase in MHC II induced by shALIX (sh1) in the HeLa-CIITA cells and their exosomes was also observed in cells that endogenously express MHC II molecules. We analysed human monocyte-derived DCs because their exosomes can induce immune responses and are currently used in a clinical trial (Viaud et al., 2011; Zitvogel et al., 1998). Blood-derived monocytes were transduced with shSCR or shALIX, differentiated to DCs with IL-4 and GM-CSF and selected with puromycin for 5 days. Untreated cells and cells treated with lipopolysaccharide (LPS) and interferon-γ (IFN-γ) to induce maturation, were analysed by western blotting: as shown in Fig. 6A, an effective depletion of ALIX (between 60 and 100%) was observed in shALIX-treated cells. MHC II content was significantly ($P<0.05$) increased in shALIX-treated immature DCs, to levels comparable with those observed in mature LPS+IFN-γ-treated cells. By contrast, in mature DCs the high level of total MHC II molecules was not further increased upon

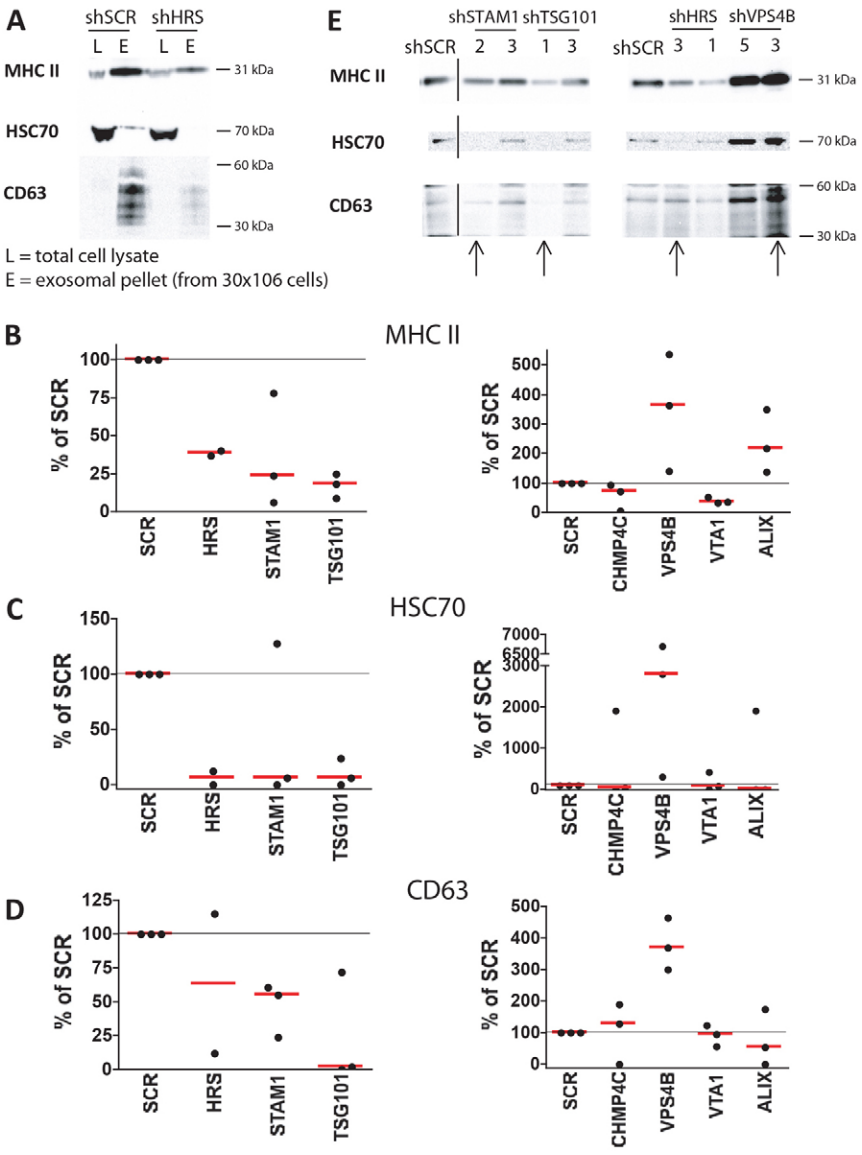

Fig. 2. Validation of the exosome-modulating genes identified by screening. Exosomes were purified by differential centrifugations and characterized by western blotting (WB). For each individual experiment, vesicles from shSCR- and other shRNA-expressing cells (sh3 for *HRS*, *CHMP4C* and *VPS4B*, sh2 for *STAM1*, sh1 for *TSG101*, *VTA1* and *ALIX*) were analysed and processed simultaneously, to ensure comparable signals. (A). Exosomes secreted by 30×10^6 cells, and total cell lysates were characterized by WB, using three different markers enriched on exosomes (MHC II, HSC70 and CD63). Results obtained with control and shHRS-treated cells are shown as an example. Quantification of MHC II (B), HSC70 (C) and CD63 (D) signal was performed with the ImageJ software; results (measured in AU) are expressed as a percentage of the control (shSCR); the red bar indicates the median, and the black line indicates the level of the control (shSCR, 100%). (E) The effect of two different shRNAs is shown for the genes for which large-scale analysis of exosome secretion confirmed the results obtained in the screen: *HRS*, *TSG101*, *STAM1*, *VPS4B*. Arrows indicate the shRNAs used in 2B–D.

ALIX depletion. This could be expected since transcription of MHC II is completely shut down in fully mature DCs (Landmann et al., 2001), thus *ALIX* silencing could not modulate mRNA transcription.

To determine whether the increase in MHC II levels observed in ALIX-depleted DCs not treated with LPS+IFN-γ was due to spontaneous maturation of the cells, we performed multicolour FACS, and analysed MHC II levels of either spontaneously mature DCs expressing high level of CD86, or immature DCs without CD86 expression (supplementary material Fig. S5A). We first observed that the percentage of spontaneously matured cells was increased in shALIX-treated DCs (supplementary material Fig. S5B), which explains part of the increase in total MHC II observed by western blotting on the bulk DC population (Fig. 6A). But when analysing only the immature DC population, ALIX depletion also clearly induced a 30–400% increase in the fluorescence intensity of surface MHC II in four out of five donors (Fig. 6B, top panel), without affecting the surface level of CD63 (Fig. 6B, lower panel). Thus the increased expression of MHC II upon *ALIX* silencing was not only observed in the model HeLa-CIITA cells, but also in antigen-presenting cells.

ALIX depletion does not increase MHC II secretion on DC exosomes

The observation that ALIX depletion increased MHC II expression in DCs led us to investigate whether this also resulted in the secretion of MHC-II-enriched exosomes. We first performed the FACS-based CD63-mediated capture assay used in the screen (see Fig. 1A). Fig. 7A shows the results obtained with immature DCs treated with shALIX from seven different donors (the same donors as in Fig. 6), expressed as a percentage of the corresponding shSCR, set to 100%. No significant increase in the signal was detected with the FACS-based assay: only two out of seven

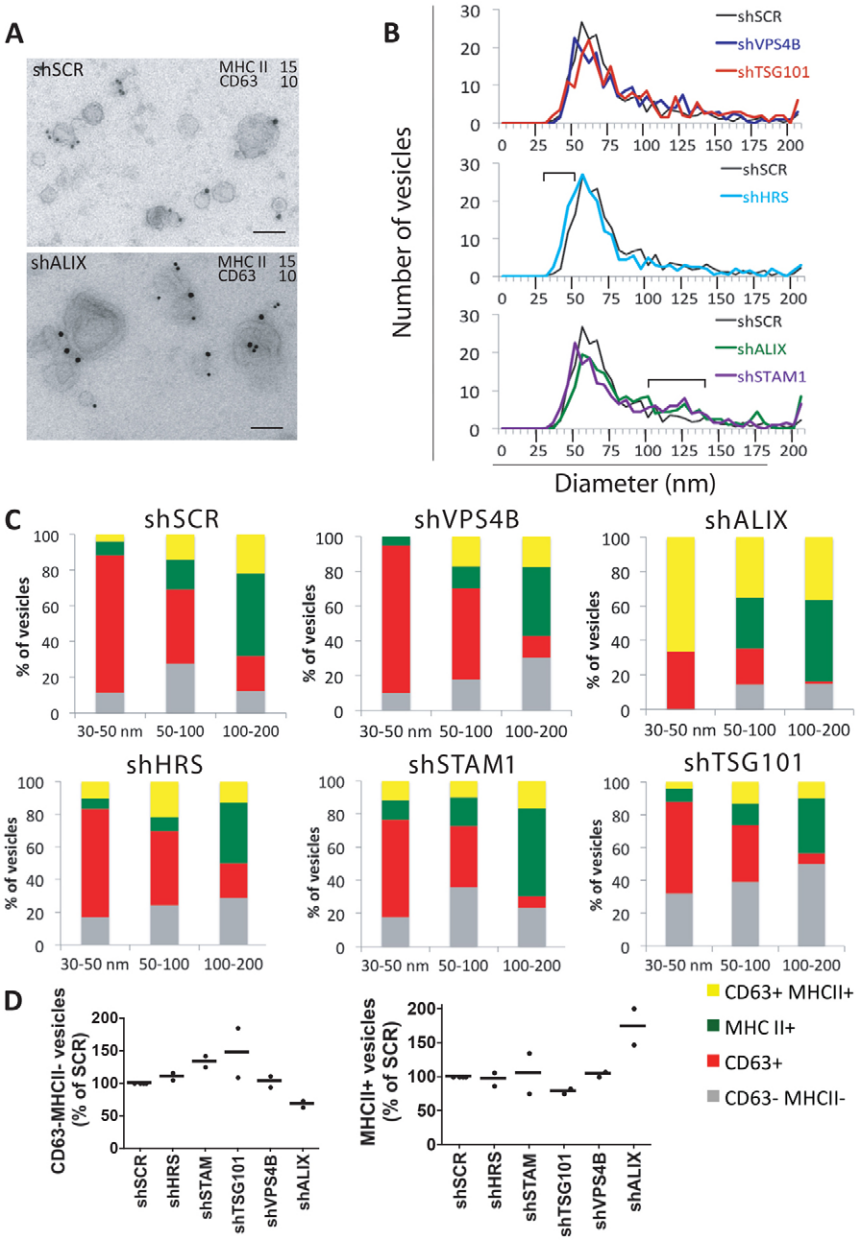

Fig. 3. Analysis of exosomes secreted by the different shRNA-treated cells by IEM. (A) Whole-mount exosomes were stained for MHC II (PAG15) and CD63 (PAG10). Images are shown for shSCR- and shALIX-derived exosomes (representative of two experiments). Scale bars: 100 nm. (B–D) The number of gold particles and the diameter of each vesicle were quantified in two to four independent experiments (2×200 vesicles for each shRNA, 4×200 for shSCR). (B) Overlays of size distribution of vesicles obtained from shRNA-treated cells (coloured lines) with shSCR vesicles (black line). Average size distribution in two to four independent experiments is shown. Upper panel (shTSG101, shVPS4B): no differences with shSCR vesicles. Middle panel (shHRS): decreased size (bracket indicates higher proportion of 25–50 nm vesicles). Lower panel (shALIX, shSTAM1): increased size (bracket indicates higher proportion of 100–140 nm vesicles). (C) The CD63 and MHCII composition is shown here for each shRNA treatment, as a percentage of vesicles with no gold particles (CD63− MHC II−), only PAG10 (CD63+), only PAG15 (MHC II+), or both (CD63+ MHC II+), for small (30–50 nm), intermediate (50–100 nm) and large (100–200 nm) particles. One representative experiment out of two. (D) Quantification of CD63− MHC I− vesicles (left panel), and MHC II+ vesicles (both CD63− and CD63+, right panel), expressed as a percentage of the control (shSCR, 100%). Individual results of two independent experiments are shown (black horizontal bar indicates the mean). shSTAM1 and shTSG101 increase and shALIX decreases the proportion of CD63− MHC II− vesicles (left panel). shTSG101 decreases and shALIX increases the proportion of MHC II+ vesicles (right panel).

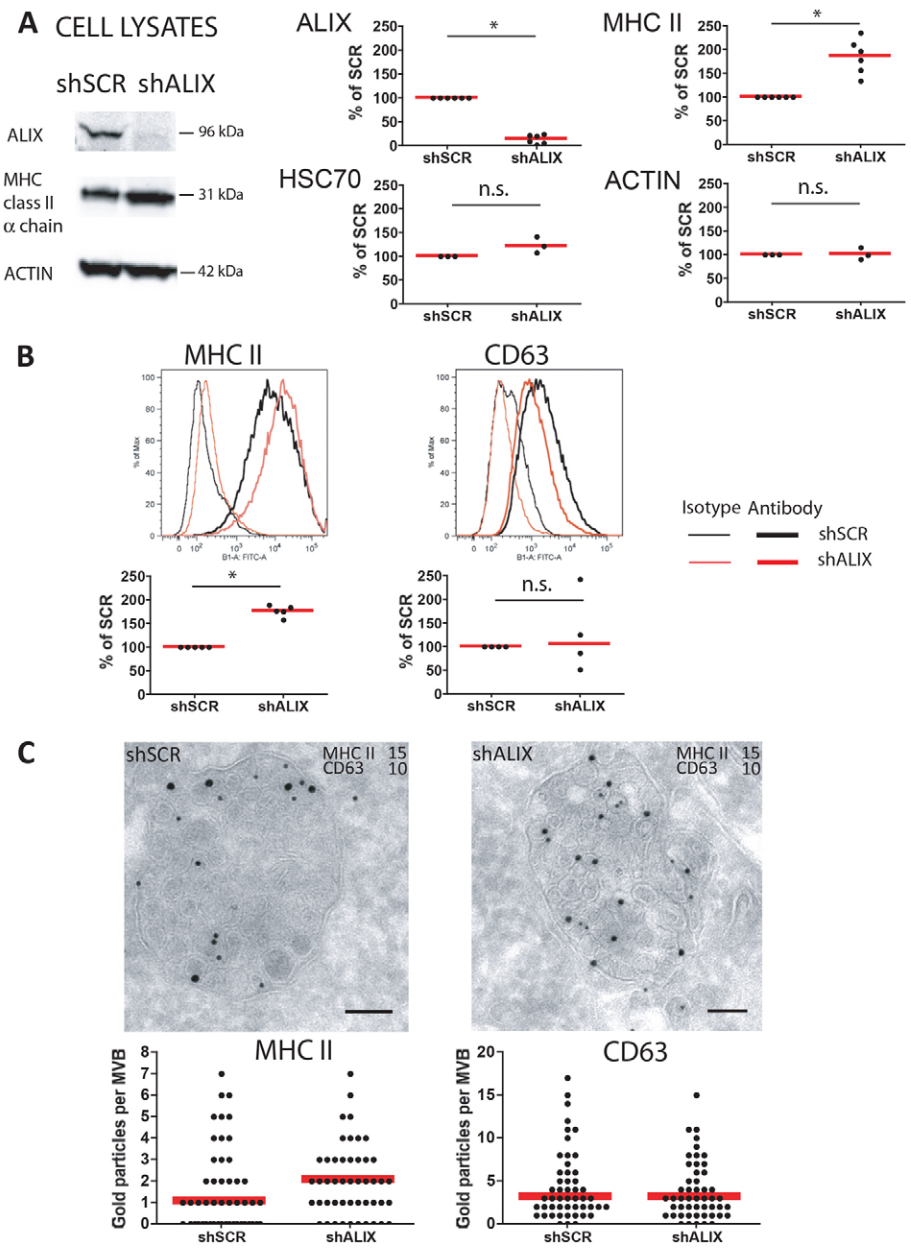

Fig. 4. Characterization of shSCR- and shALIX-treated cells. (A) Western blotting of total cell lysates (100 µg/lane); staining for ALIX, MHC II and ACTIN is shown. Quantifications of six independent experiments (right panel) show the downregulation of ALIX and the increase of MHC II in shALIX-treated cells compared with the control, and no difference in the reference proteins HSC70 and actin; results are expressed as a percentage of control (AU) and the red bar indicates the median. (B) FACS analysis of control and shALIX-treated cells (top panel), and graph of the mean fluorescence intensity (MFI) of the markers MHC II and CD63. Results are shown as the percentage of the control MFI for four or five independent experiments (bottom panel). (C) IEM of ultrathin cryosections of shSCR- (top left panel) or shALIX- (top right panel) treated cells, with labelling for MHC II (PAG15) and CD63 (PAG10). The number of MHC II (bottom left panel) and CD63 (bottom right panel) gold particles quantified on 50 individual MVBs for each condition is shown; the red bar indicates the median. Wilcoxon signed-rank test; $*P<0.05$; n.s., not significant. Scale bars: 100 nm.

experiments (donors 3 and 6) showed a slight increase, albeit much lower (less than 50%) than that for HeLa-CIITA cells (around 75–100%). The other experiments showed no effect (donor 4), or a decrease of 50% or higher (donors 1, 2, 5 and 7). These results suggest that the relative composition of MHC II, CD63 and CD81 in exosomes secreted by DCs could be different from that of HeLa-derived exosomes, and different between donors. We thus tested by IEM DC-derived EVs obtained by 100,000 ***g*** ultracentrifugation, as done for HeLa-CIITA (Fig. 7B). Vesicles obtained from three independent DC preparations not treated with shRNA were analysed: pooled results are shown in Fig. 7, and individual results in supplementary material Fig. S6. The first striking difference was that EVs of human DCs were of heterogeneous sizes, with equal proportions of vesicles of 50–100 and of 100–200 nm, whereas HeLa-CIITA-derived EVs were mainly 50–100 nm (Fig. 7C,D). In addition, even among the small DC-derived vesicles, fewer bore CD63 than the small HeLa-CIITA vesicles (Fig. 7D), thus questioning their exosomal nature as defined in this study. Finally, although the proportion of EVs bearing both CD63 and MHC II was similar in DC and HeLa-CIITA (~20%), we noticed that the former EVs bore proportionally much more MHC II, with on average two 15 nm (=MHC II) for one 10 nm (=CD63) gold particles, whereas in HeLa-CIITA vesicles the ratio was closer to 1/1 (Table 2). The already high level of MHC II molecules present on vesicles secreted by normal immature DCs probably explains why the increased cellular expression of MHC II induced by shALIX does not induce an increase in MHC II association with DC-derived EVs. Thus, our results show that ALIX modulates MHC II levels in two different cell types, but also highlight differences in the size and composition of EVs purified with the same procedures from different cell types.

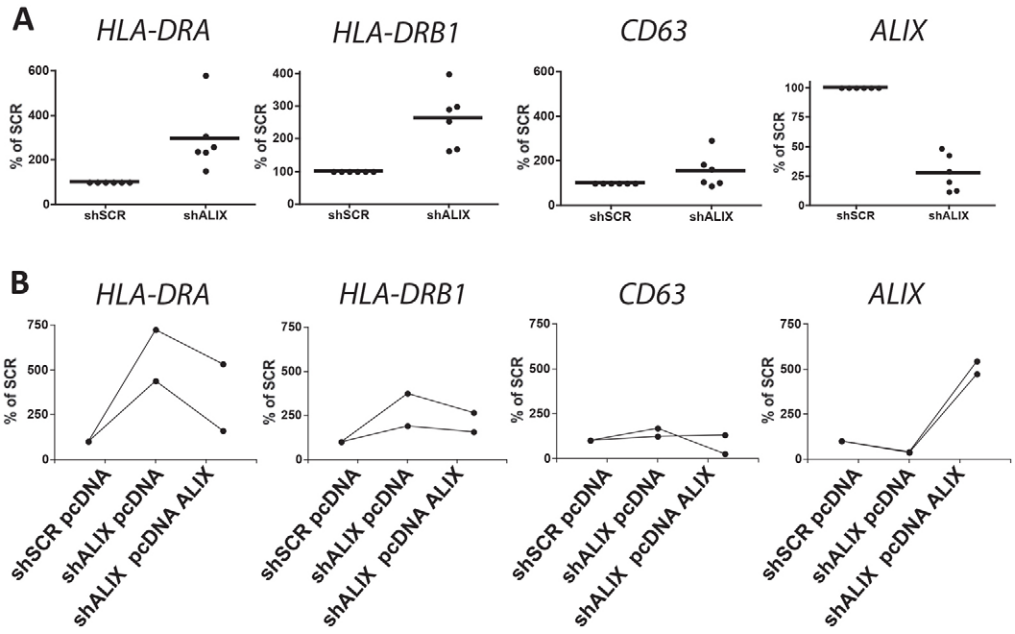

Fig. 5. Effect of *ALIX* silencing on MHC II mRNA expression.
(A) Quantitative real-time PCR (qRT-PCR) measurement for MHC II alpha chain (HLA-DRA), beta chain (HLA-DRB1), CD63 and ALIX in shSCR- and shALIX-treated cells.
(B) Quantification by qRT-PCR of expression of the same genes as in A in shALIX-treated cells upon re-expression of ALIX cDNA. shALIX-treated cells transfected with empty pcDNA or shRNA-resistant *ALIX*-expressing pcDNA were compared with shSCR cells transfected with empty pcDNA (=100%). Individual points obtained in six (A) and two (B) independent experiments are shown.

Discussion

Studies in reticulocytes (Harding et al., 1983; Pan et al., 1985), EBV-B lymphocytes (Raposo et al., 1996; Wubbolts et al., 2003) and DCs (Zitvogel et al., 1998; Buschow et al., 2009), as well as more recent findings in the HeLa-CIITA cell model (Ostrowski et al., 2010) support an endosomal origin of exosomes. Because they correspond to the internal vesicles of MVBs, candidate targets for intervention on their biogenesis and secretion are mechanisms thought to be involved in cargo sequestration at the endosomal membrane and vesicle budding and scission. The discovery that the ESCRT machinery is involved in MVB formation (Henne et al., 2011; Raiborg and Stenmark, 2009) opened a new avenue to interfere with the formation of ILVs and thereby exosome secretion. However, the evidence that ESCRT-independent mechanisms also operate for the biogenesis of MVBs and sorting of components to ILVs (Theos et al., 2006; Trajkovic et al., 2008; Stuffers et al., 2009; van Niel et al., 2011) suggested that these mechanisms could be broader and therefore more complex and redundant that initially envisioned.

In this study we set out to investigate, for the first time, the involvement of a large panel of ESCRT components (23 genes in total) in exosome biogenesis and secretion in HeLa-CIITA cells. For this purpose, we performed a screening using a FACS-based assay, which allowed relative quantification of exosomes secreted into the supernatant of cells treated with small hairpin RNA. Since exosomes have been previously described as enriched in tetraspanins and MHC II molecules, we designed this assay to quantify the population of vesicles bearing CD63 and either CD81 or MHC II, which we assumed would correspond most specifically to vesicles originating from endosomes. Of note, this readout obviously provides information on a selected fraction of all secreted exosomes, because it does not take into account vesicles bearing CD63 but none of the other two proteins. In addition, combined detection of two distinct proteins, MHC II and CD81, to allow relative quantification of captured exosomes during the screen may have masked subtle effects of some shRNA, e.g. on specific incorporation of only one of these proteins in exosomes, or on specific release of a subpopulation of vesicles bearing only one of them. As for any shRNA screen, we can only firmly conclude that the four genes for which strong positive effects were observed in the screen, and which were then further validated by additional complementary methods (western blotting, quantitative IEM analysis of exosomes and of MVBs) are involved in exosome biogenesis: *HRS*, *TSG101*, *STAM1* and *VPS4B*. We cannot exclude that some of the ESCRT genes, those that did not reach the selection criteria in our initial screen, may still be involved at any other step of exosome biogenesis, or need to act in concert resulting in no phenotype when individually silenced.

Our IEM analysis of exosomes secreted by HeLa-CIITA revealed the presence not only of vesicles double positive for CD63 and MHC II, but also of vesicles bearing only MHC II or CD63, and vesicles that appear negative for both markers (but could be expressing low amounts that are under the limits of detection by IEM). Exosomes positive for MHC II and CD63 were 10–20% of all secreted vesicles in most conditions employed in this study. It is likely that other exosomal markers such as CD81 also have a heterogeneous distribution in exosomes. Our assays together highlight and extend previous reports (Bobrie et al., 2012; van Niel et al., 2001) that cells secrete a heterogeneous population of exosomes with different sizes and composition. This fully corroborates the observations that cells contain different MVBs and that within MVBs, ILVs are not all similar in morphology and composition (Fevrier et al., 2004; Möbius et al., 2002; White et al., 2006). In addition, we also show here that EVs recovered from human primary DCs are more heterogeneous in size and protein composition than those secreted by HeLa-CIITA (Fig. 7), and also vary from one donor to the other (supplementary material Fig. S6). These observations suggest that DCs from different donors secrete variable proportions of vesicles derived either from intracellular compartments (exosomes) or possibly from the plasma membrane. Thus, proteins specifically enriched in the different subpopulations of vesicles will have to be identified in the future, to allow the development of other capture-based assays to

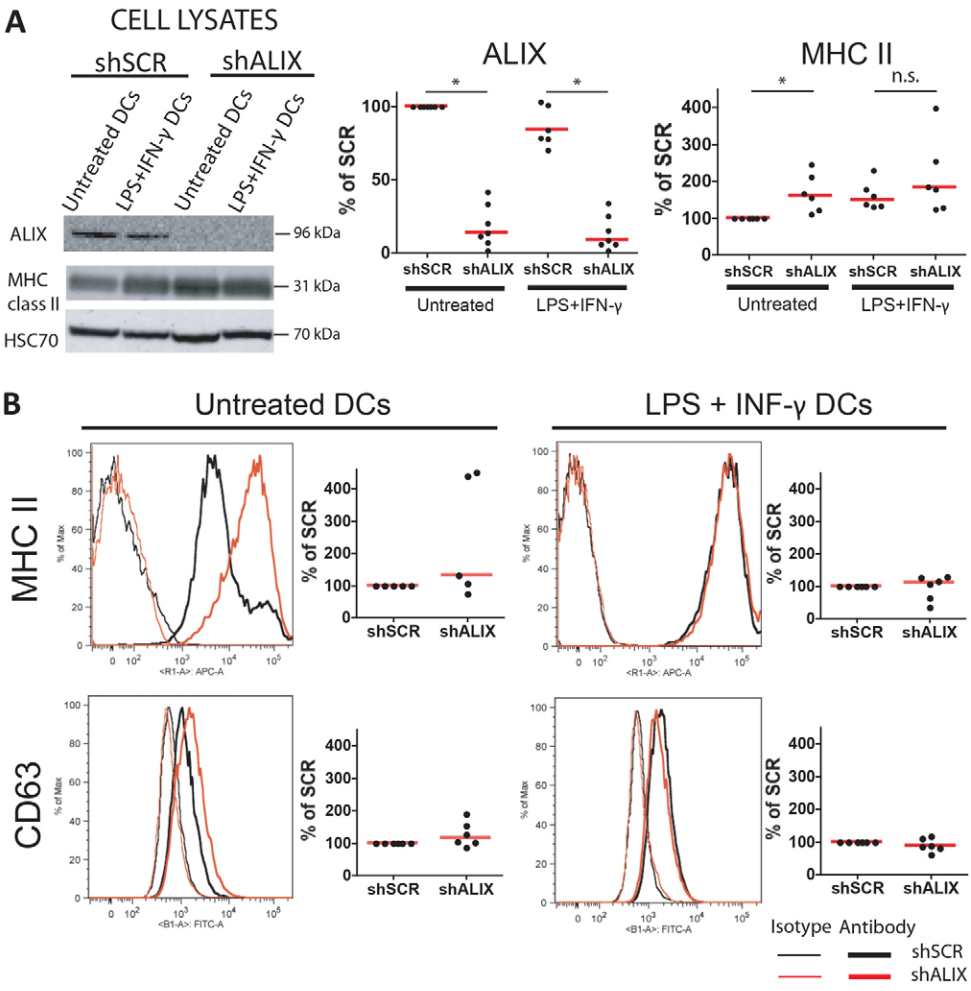

Fig. 6. Characterization of shSCR- and shALIX-treated human primary DCs. (A) Western blotting of total cell lysates from untreated DCs or LPS+IFN-γ-treated DCs; staining for ALIX, MHC II and HSC70 is shown. Quantifications of band signal performed on western blots of cell lysates from independent donors (right panels) show the downregulation of ALIX and the increase of MHC II in shALIX-treated cells as compared with the control. Results (AUs) are expressed as a percentage of the untreated control (untreated shSCR). (B) FACS analysis of control and shALIX-treated cells with markers MHC II (top) and CD63 (bottom) and graph of the MFI expressed as percentage of the control (MFI marker – MFI isotype control) for independent donors; untreated DCs (left panel, MHC II levels analysed only in CD86-negative immature DCs), or LPS+IFN-γ-treated DCs (right panel). Wilcoxon signed-rank test; $*P<0.05$; n.s., not significant.

identify the molecular machinery involved in their respective secretion.

Our work conclusively shows that silencing of genes for two components of ESCRT-0 (*HRS*, *STAM1*) and one of ESCRT-I (*TSG101*), as well as a late acting component (*VPS4B*) induced consistent alterations in exosome secretion. Previous studies on an oligodendrocytic cell line secreting PLP in association with exosomes highlighted a formation and release process independent of ESCRT function but requiring the production of the lipid ceramide by a type II sphingomyelinase (Trajkovic et al., 2008). In this study, silencing of *HRS*, *TSG101*, *ALIX* and *VPS4* did not alter consistently the sequestration of PLP in ILVs of MVBs, although it reduced the trafficking of epidermal growth factor (EGF) and its receptor to MVBs. However, our data clearly show that secreted exosomes are heterogeneous in terms of their size and cargo, and since this previous study only followed one population (i.e. PLP-containing exosomes) in a given cell type, it is in our opinion difficult to extrapolate that all exosome populations are ESCRT independent. As suggested before by an extensive proteomic analysis of exosomes secreted at different stages of reticulocyte maturation (Carayon et al., 2011), different cargos can be sorted by distinct mechanisms, which contributes to such heterogeneity of ILVs. Our results indicate that loss of function of selected ESCRT components, which in some cases decreases (HRS, STAM1, TSG101) or increases (VPS4B) the amount of vesicles and cargo associated with vesicles, also modulates the nature and protein contents of the vesicles. Silencing of *HRS*, *STAM1* and *TSG101* decreased the number of vesicles and associated proteins (MHC II, CD63) but the three ESCRT components seemed to operate differently during the biogenesis or secretion of the different subpopulations of EVs. Upon HRS depletion, secretion of vesicles of between 50 and 100, and 100 and 200 nm diameter was slightly reduced as compared with control cells, suggesting that HRS is not required for formation and secretion of the vesicles smaller than 50 nm. Although STAM1 is also part of the ESCRT-0 complex, its depletion decreased the population of vesicles with diameters between 30 and 50 and 50–100 nm, suggesting that STAM1, in contrast to HRS, is required for formation and secretion of the smallest vesicles. We cannot exclude that part of the remaining vesicles are not endosome-derived exosomes but rather vesicles that could be derived from the plasma membrane, and that STAM1 loss-of-function increases their budding and release. Depletion of TSG101, and to a lesser extent STAM1, resulted in a modification of the overall protein content of exosomes, as evidenced by an increase in vesicles negative for both CD63 and MHC II in all size categories, suggesting that TSG101 and STAM1 are rather required for targeting these cargoes into ILVs.

Thus, interfering with the function of some early components of the ESCRT machinery decreases exosome production but the

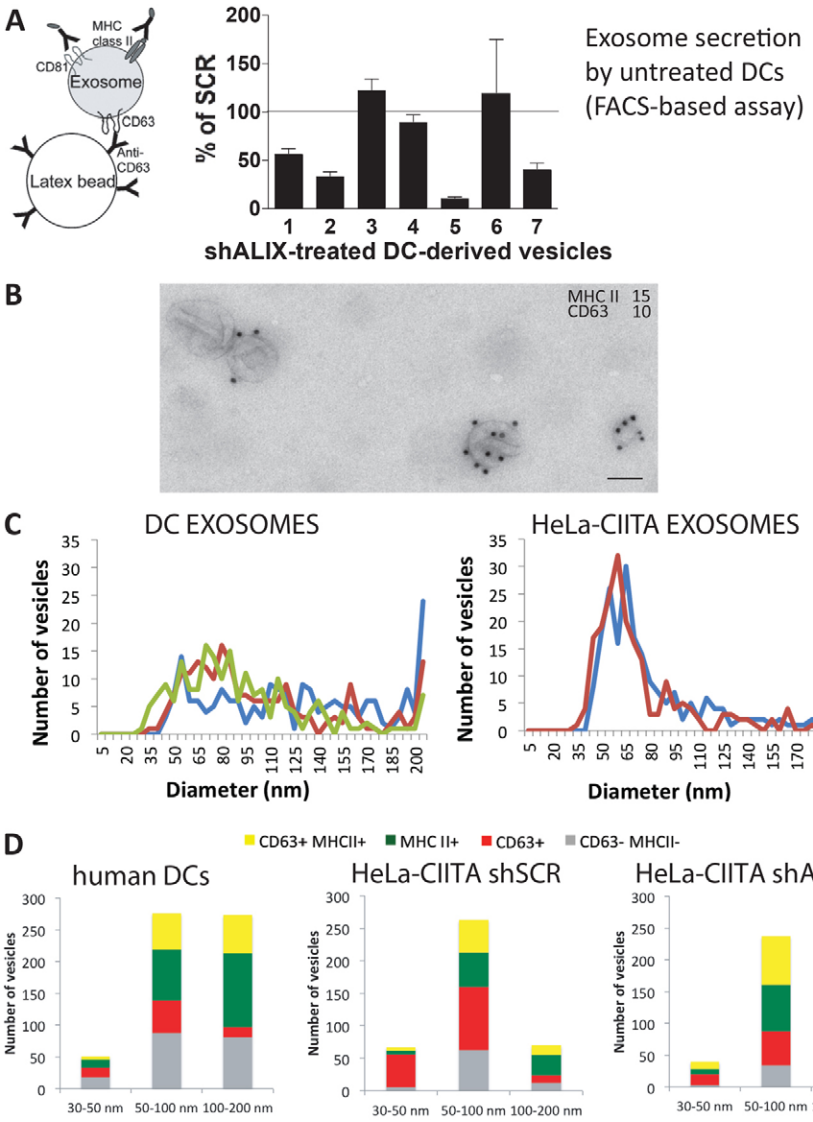

Fig. 7. IEM analysis of exosomes secreted by human monocyte-derived DCs. (A) Exosome secretion by shALIX-expressing DCs from seven donors (data on maturation status of DCs from donors 1 and 2 were not available, and are thus not shown in supplementary material Fig. S5): exosomes were quantified by trapping on anti-CD63-coated beads and staining with anti-CD81 and anti-HLA-DR antibodies. Results (AUs) are expressed as a percentage of the control DCs (shSCR from the same donor; values are means ± s.d. from one experiment performed in triplicate for each donor. The black horizontal line indicates the level of the control (shSCR, 100%). (B) Whole-mount exosomes were stained for MHC II (PAG15) and CD63 (PAG10). Representative image with exosomes obtained from non-shRNA-treated DCs. Both the number of gold particles and the diameter were quantified for 200 vesicles per condition. Scale bar: 100 nm. (C) Size distribution of exosomes secreted by DCs (left panel, three independent experiments) and by HeLa-CIITA cells (right panel, two independent experiments). (D) Number of vesicles with no gold particles (CD63− MHC II−), only PAG10 (CD63+), only PAG15 (MHC II+), or both (CD63+ MHC II+), for small (30–50 nm), intermediate (50–100 nm) and large (100–200 nm) vesicles secreted by hDCs (left panel, pool of three experiments), control HeLa-CIITA cells (middle panel, pool of two experiments), and HeLa CIITA cells silenced for *ALIX* (right panel, pool of two experiments).

nature of the vesicles that are still present in the supernatants is different. This is consistent with the model that ESCRTs act sequentially in cargo sequestration and vesicle formation, which consequently impacts on endosome maturation including the formation of ILVs of endosomes. As shown by Razi and Futter, the depletion of HRS and TSG101 impact differently in the maturation of MVBs (Razi and Futter, 2006). Unexpectedly, silencing of *VPS4B* increased exosome secretion, as monitored during the screen, but also after evaluation of the amount of proteins associated with exosomes. Depletion of VPS4B increased secretion of all markers associated with exosomes (CD63, MHC II, HSC70), but also increased exosome-independent secretion of ovalbumin, suggesting a general effect on the secretory pathway. Finally, depletion of ALIX increased the amount of MHC II in cells and consequently in the secreted vesicles, and increased the proportion of medium-sized and larger vesicles (50–100/100–200 nm), indicating that ALIX may control the nature of secreted vesicles. A recent report showed that ALIX is required for the sequestration of syndecans within exosomal membranes through its interaction with syntenin, and

Table 2. MHC class II and CD63 labelling on double-positive vesicles purified from different secreting cells

Cell type	Amount of MHC II gold particles on double-positive vesicles (mean ± s.e.m.)	Amount of CD63 gold particles on double-positive vesicles (mean ± s.e.m.)
HeLa CIITA shSCR	1.4±0.2	1.6±0.1
HeLa CIITA shSCR	1.4±0.2	1.8±0.2
HeLa CIITA shALIX	2.2±0.2	1.7±0.1
HeLa CIITA shALIX	2.0±0.2	1.9±0.2
hDCs donor A	4.4±1.2	1.8±0.2
hDCs donor B	2.7±0.6	1.8±0.2
hDCs donor C	2.2±0.3	1.5±0.1

that ALIX depletion results in reduced exosome secretion (Baietti et al., 2012). Our results do not challenge these findings but rather put forward the idea that, depending on the cell types and the cargoes associated with different exosome subpopulations, the mechanisms involved may slightly change. Indeed, when we analysed exosome secretion by DCs, our CD63-mediated exosome capture assay failed to detect increased secretion of MHC-II-bearing exosomes upon ALIX depletion. On the contrary, a decreased secretion of EVs by the majority of donors was observed (Fig. 7A). This could indicate either that EVs secreted by ALIX-inactivated DCs did not present an increase in MHC II at their surface despite the overall overexpression of MHC II in the secreting cells, or that secretion of CD63-bearing exosomes was decreased in ALIX-impaired DCs, which was compensated by the increased amount of MHC II on these exosomes. In any case, the difference between DCs and MHC II-expressing HeLa, or non-MHC-II-expressing human tumours (Baietti et al., 2012) might imply that ALIX impacts on exosome biogenesis, but that different mechanisms are exploited by these very different cell types to secrete EVs. In particular, a tight balance of mechanisms probably operates at the endosomal membrane, controlling protein sorting to distinct ILVs subpopulations that may in some cases have different fates (van Niel et al., 2011). It will be important in the future to elucidate the molecular requirements for these different exosomal cargoes within the same cell type.

Our observations that the silencing of *ALIX* increased MHC II expression on secreted EVs led us to further investigate the alterations of MHC II expression in the secreting cells. FACS analysis clearly indicated a consistent increase of MHC II at the cell surface (but not of CD63) and IEM revealed numerous MVBs densely labelled for MHC II. Therefore, ALIX depletion increases MHC II expression in the cells. In monocyte-derived human DCs, as in HeLa-CIITA, silencing of *ALIX* induced an increase of total cellular MHC II (Fig. 6). Given the known functions of ALIX in MVB formation, and the previously described mechanism of MHC II degradation in murine DCs by oligo-ubiquitylation, leading to targeting to internal vesicles of MVBs and degradation (Shin et al., 2006; van Niel et al., 2006), our initial hypothesis was that ALIX could promote this degradation pathway, to limit the half-life of MHC II. Preliminary experiments to address this question did not allow us to confirm this hypothesis (data not shown). Instead we demonstrated an increase in the mRNA level of genes of the MHC II machinery in shALIX-expressing cells. Our results unravel a new role for ALIX in the transcriptional control or mRNA stability of MHC II expression. A recent study (Lambert et al., 2012) showed, by yeast two-hybrid screening, that the transcription factor Hoxa1 can interact with ALIX. Microscopy experiments suggested that this interaction occurs in intracellular compartments of a vesicle-like nature. It is therefore possible that ALIX may exert its function in the control of MHC II expression by interacting with transcription factors that bind the MHC II promoters, either directly or by controlling the CIITA transactivator.

In conclusion, our findings altogether reinforce the concept that cells contain different subpopulations of MVBs and secrete a heterogeneous population of exosomal vesicles. Whereas ESCRT-independent mechanisms are involved in MVB and exosome biogenesis (Trajkovic et al., 2008; van Niel et al., 2011), our observations and recent reports (Baietti et al., 2012; Tamai et al., 2010) show that the formation and secretion of a population of exosomes also rely on the function of ESCRTs and accessory proteins, and that only selected components may be involved in protein sorting and the formation of the ILVs fated to be secreted as exosomes. These observations will certainly contribute to our understanding of the mechanisms involved in exosome formation and will open an avenue for modulating the nature of exosomes and their composition.

Materials and Methods

Cells and reagents

HeLa-CIITA OVA cells [subclone B6H4 (Ostrowski et al., 2010)] were cultured in DMEM containing 4.5 g/l glucose (Life Technologies) 10% fetal calf serum (FCS, Gibco or PAA), 100 IU/ml penicillin and 100 µg/ml streptomycin (Gibco), 300 µg/ml hygromycin B (Calbiochem) and 500 µg/ml geneticin (Life Technologies). Medium depleted of FCS exosomes (exosome-depleted medium) was obtained by overnight ultracentrifugation of complete medium at 100,000 ***g*** (Théry et al., 2006).

Lentiviruses expressing shRNA and a puromycin resistance gene were obtained from the RNAi consortium (TRC) and produced as described previously (Moffat et al., 2006). As a control, the scrambled sequence of shRNA for GFP (not targeting any human gene) was used (shSCR). Sequences of shRNA are given in supplementary material Table S1. For rescue experiments, a cDNA encoding human ALIX with silent mutations in the shRNA-binding domains (supplementary material Table S1) was designed and purchased from Genscript, cloned in the pcDNA3.1/Zeo expression plasmid (Life Sciences).

Antibodies used for FACS analysis of bead-captured exosomes were: mouse anti-human CD63 (clone FC-5.01, Zymed; or clone H5C6, BD Biosciences) and goat anti-OVA (ICN) for coupling to beads; PE-conjugated anti-HLA-DR (clone L243, BD Biosciences), anti-CD81 (clone JS-81, BD Biosciences); rabbit anti-OVA (Sigma) coupled to Alexa Fluor 488 according to the manufacturer's instructions (DyLight 488 Antibody Labelling Kit, Pierce). For FACS analysis of cells: anti-HLA-DR (L243) or anti-CD63 (H5C6) followed by Alexa Fluor 488 anti-mouse (Molecular Probes). Antibodies used for western blotting were: mouse anti-TSG101 (Genetex); rat anti-HSC70 (Stressgen); mouse anti-CD63 (FC-5.01 or H5C6), anti-HLA-DR (clone 1B5), rabbit anti-VPS4B (Abcam), goat anti-HRS (Santa Cruz) and rabbit anti-VTA1 (Abcam); HRP-conjugated secondary antibodies (Jackson Immunoresearch). Antibodies used for IEM were: rabbit anti-HLA-DR (H. Ploegh, Whitehead Institute, Cambridge, MA), mouse anti-HLA-DR (L243) and mouse anti-CD63 (Zymed). Protein-A–gold conjugates were purchased from Cell Microscopy Centre (Utrecht University, Netherlands).

Screening procedure

For each independent experiment, HeLa-CIITA-OVA were newly infected with shRNA-expressing lentiviruses. The screen was performed as previously described (Ostrowski et al., 2010), with some minor differences: aldehyde-sulfate beads (Invitrogen) were coated with anti-CD63 or anti-OVA antibodies by incubating 140 µg of antibody with 70 µl beads, and after incubation with cell culture supernatants they were stained for flow cytometry with PE-anti-HLA-DR (1:50), PE-anti-CD81 (1:100) and Alexa-Fluor-488 anti-OVA (1:200) and analysed using a MACSQuant flow cytometer (Miltenyi Biotec). Three independent experiments were performed, in which the effect of shSCR and each gene-specific shRNA was analysed in triplicate. To exclude all non-specific effects on vesicle release due to shRNA- or puromycin-induced cell death, cell numbers were quantified in each well using Cell Titer Blue reagent (Promega) at the end of the exosome-production period, and only wells containing the same number of cells (±20%) as the control shSCR were considered for further analysis. In each experiment, the basal level of exosome or OVA secretion (control) was calculated as the mean arbitrary units (AU) of the triplicate wells of each sample type and the values expressed as a percentage of control value. The mean of nine values from three independent experiments is shown in Fig 1; supplementary material Figs S1 and S2.

RNA extraction and real-time qPCR

RNA was extracted from cells in each well with the RNA XS kit or from 5×10^5 to 1×10^6 cells with the RNA II kit (Macherey Nagel). Reverse transcription and quantitative real-time PCR were performed as described previously (Bobrie et al., 2012), using primers purchased from Qiagen (QuantiTect Primer Assay). Gene expression was normalized to the level of *GAPDH* or actin expression.

Exosome purification

For each condition 5×10^7 cells were plated in exosome-depleted medium and incubated for 48 hours. Supernatants were then harvested and exosome purification was performed as previously described (Théry et al., 2006). The number of cells after cell detachment from all the dishes was determined using an automated Countess cell counter (Life Technologies), and was similar in all experimental conditions. Supernatants were centrifuged at 300 ***g*** for 5 minutes to

eliminate floating cells, at 2000 ***g*** for 20 minutes to remove cell debris, and at 10,000 ***g*** for 40 minutes to separate microvesicles. An ultracentrifugation step at 100,000 ***g*** for 90 minutes in a 45Ti rotor was performed to obtain exosomes, followed by a washing step in PBS to eliminate contaminating proteins. Exosomes were resuspended in 100 µl PBS, and protein content was measured by MicroBCA (Pierce) in the presence of 2% SDS.

Western blotting

A volume of exosomes secreted by 30×10^6 cells, or 100 µg of total cell lysate were used for western blotting. Western blotting and quantifications were performed as previously described (Bobrie et al., 2012). For each independent experiment, vesicles secreted by the different shRNA-expressing cells were analysed on gels and membranes processed simultaneously.

Flow cytometry analysis

For surface staining, cells were harvested and incubated with anti-MHC II or -CD63 antibody (2 µg/ml) for 30 minutes on ice, followed by anti-mouse Alexa Fluor 488 antibody (1/200) for 20 minutes on ice, and analysis on a MACSQuant flow cytometer.

Electron microscopy

Exosomes resuspended in PBS were deposited on formvar–carbon-coated copper/palladium grids for whole-mount IEM analysis as previously described (Théry et al., 2006; Raposo et al., 1996). For double labelling, samples on grids were successively incubated with mouse anti-MHC II, 15 nm protein-A–gold (PAG) (PAG15), 1% glutaraldehyde (Electron Microscopy Sciences), anti-CD63, PAG10 and glutaraldehyde, before being contrasted and embedded in a mixture of methylcellulose and uranyl acetate.

Transduced cells were fixed in 0.2 M phosphate buffer (pH 7.4) with 2% PFA and 0.125% glutaraldehyde for 2 hours at room temperature. Cells were then processed for ultrathin cryosectioning as previously described (Raposo et al., 2001), and labelled with rabbit anti-MHC II (1/200) or anti-CD63 (2 µg/ml) antibodies, followed by PAG15 and PAG10, respectively.

Samples were observed with a CM120 Twin FEI electron microscope (FEI Company, Eindoven, The Netherlands) at 80 kV, and digital images were acquired with a numeric camera (Keen View, Soft Imaging System, Germany). Quantification was performed with the iTEM software (Soft imaging System). For exosome quantifications, one area of the grid was chosen randomly at low magnification and one image was obtained by multiple image acquisition (comprising nine individual micrographs). For all cell analysis after immunogold labelling on ultrathin cryosections, labelling for MHC II and CD63 in MVBs was quantified in 50 compartments chosen randomly in electron micrographs acquired at the same magnification.

Rescue experiments

HeLa-CIITA-OVA cells were infected with shRNA-expressing lentiviruses, treated 36 hours later with 5 µg/ml puromycin, and plated after 36 hours in six-well plates (2.5×10^5 cells/well). The next day, cells were transfected with the *Trans*IT-LT1 transfection reagent (Mirus) and 2.5 µg/well of pcDNA3.1/Zeo (Life Sciences) or the same plamid expressing human *ALIX* with silent mutations in the shRNA-binding domains, according to the manufacturer's recommendations. Cells were harvested 72 hours after transfection for RNA extraction and subsequent reverse transcription and qRT-PCR (see above).

Dendritic cell transduction and FACS assay

Monocyte-derived DCs were obtained from blood samples of healthy human donors. This study was conducted according to the Helsinki Declaration, with informed consent obtained from the blood donors, as requested by our Institutional Review Board. PBMC were isolated by density gradient centrifugation (LymphoPrep, Axis-Shield), $CD14^+$ monocytes were obtained by magnetic sorting (Miltenyi Biotec) and cultured in RPMI 1640 (Gibco) supplemented with 10% FCS (Biowest), 50 mM 2-ME, 10 mM HEPES, 100 IU/ml penicillin and 100 µg/ml streptomycin (Gibco), with 50 ng/ml IL-4 and 100 ng/ml GM-CSF (Miltenyi Biotec).

Monocytes were transduced with shSCR or shALIX according to the protocol by Satoh and Manel (Satoh and Manel, 2013). Briefly, HEK293T cells were transfected with plasmids pLKO.1, pΔ8.9, pCMV-VSV-G and TransIT-LT1 transfection reagent (Mirus Bio) to generate a lentiviral vector carrying an shRNA sequence and the puromycin resistance gene; or with plasmids $pSIV3^+$ and pCMV-VSV-G to generate helper particles containing the Vpx protein, which overcomes the blocking of lentiviral infections normally observed in monocyte-derived DCs (Goujon et al., 2006). Fresh monocytes were incubated with equal volumes of both particles and 8 µg/ml protamine for 48 hours, and then incubated with fresh medium with 2 µg/ml puromycin for 72 hours. Immature DCs thus obtained were incubated at 2×10^5 cells per well in exosome-depleted medium for 24 hours (in triplicate) to detect secreted exosomes by trapping on beads followed by staining for flow cytometry, as described above. Maturation was induced by treating DCs with LPS (1 µg/ml; Sigma) and IFN-γ (2500 IU/ml; Miltenyi Biotec). To check DC differentiation and maturation status, multicolour FACS analysis was performed, using anti-HLA-DR-APC/anti-CD86-FITC/anti-CD81-PE, anti-CD63-FITC/anti-CD80-PE, or anti-CD14-PE/anti-CD1a-PECy5 (1/100, BD Biosciences except anti-CD63, BioLegend) or the corresponding isotype controls (1/100, BD Biosciences).

Statistical analysis

Statistical tests were performed with GraphPad Prism software (GraphPad Software, Inc.). Screening results were analysed by one-way ANOVA followed by Tukey's post-hoc test. Western blot and FACS analyses comparing shRNA-treated cells with shSCR-treated cells, were analysed by a Wilcoxon signed-rank test comparing the medians to a hypothetical value of 100. Percentages of CD86-positive DCs (supplementary material Fig. S5B) were compared by a paired *t*-test. Values are shown as means ± s.d. in Figs 1, 7; supplementary material Figs S1 and S2, or as median in Figs 2, 4, 5, 6 and supplementary material Fig. S4.

Acknowledgements

The expertise of the PICT IBiSA Imaging Facility and the use of the Nikon Imaging Center at the Institut Curie were crucial for this work.

Author contributions

M.C., C.T. and G.R. designed the experiments, analysed data and wrote the article. M.C., C.M., J.K. and J.V. performed experiments. G.V.N., P.B., N.M. and L.F.M. analysed data, provided reagents, and read and revised the article.

Funding

This work was supported by Institut National de la Santé et de la Recherche Médicale, Centre National de la Recherche Scientifique and Institut Curie, the Agence Nationale de la Recherche (grant numbers: ANR-09-BLANC-0263 to C.T., G.R. and P.B., ANR-10-IDEX-0001-02 PSL* and ANR-11-LABX-0043 to C.T., N.M. and P.B.), the Fondation de France [Annual Award 2010 to C.T.], the Institut National du Cancer [2008-PL-BIO to C.T. and G.R.], ATIP-Avenir program to N.M., European FP7 Marie Curie Actions grant to N.M., Ville de Paris Emergence program to N.M., European Research Council grant to N.M., and Fondation ARC (SL220100601359) to GR and [DOC20110603085] to M.C.

supplementary material available online at
http://jcs.biologists.org/lookup/suppl/doi:10.1242/jcs.128868/-/DC1

References

Baietti, M. F., Zhang, Z., Mortier, E., Melchior, A., Degeest, G., Geeraerts, A., Ivarsson, Y., Depoortere, F., Coomans, C., Vermeiren, E. et al. (2012). Syndecan-syntenin-ALIX regulates the biogenesis of exosomes. *Nat. Cell Biol.* **14**, 677-685.

Bobrie, A., Colombo, M., Raposo, G. and Théry, C. (2011). Exosome secretion: molecular mechanisms and roles in immune responses. *Traffic* **12**, 1659-1668.

Bobrie, A., Colombo, M., Krumeich, S., Raposo, G. and Théry, C. (2012). Diverse subpopulations of vesicles secreted by different intracellular mechanisms are present in exosome preparations obtained by differential ultracentrifugation. *J. Extracell. Vesicles* **1**, 18397.

Bowers, K., Piper, S. C., Edeling, M. A., Gray, S. R., Owen, D. J., Lehner, P. J. and Luzio, J. P. (2006). Degradation of endocytosed epidermal growth factor and virally ubiquitinated major histocompatibility complex class I is independent of mammalian ESCRTII. *J. Biol. Chem.* **281**, 5094-5105.

Buschow, S. I., Liefhebber, J. M., Wubbolts, R. and Stoorvogel, W. (2005). Exosomes contain ubiquitinated proteins. *Blood Cells Mol. Dis.* **35**, 398-403.

Buschow, S. I., Nolte-'t Hoen, E. N., van Niel, G., Pols, M. S., ten Broeke, T., Lauwen, M., Ossendorp, F., Melief, C. J., Raposo, G., Wubbolts, R. et al. (2009). MHC II in dendritic cells is targeted to lysosomes or T cell-induced exosomes via distinct multivesicular body pathways. *Traffic* **10**, 1528-1542.

Carayon, K., Chaoui, K., Ronzier, E., Lazar, I., Bertrand-Michel, J., Roques, V., Balor, S., Terce, F., Lopez, A., Salomé, L. et al. (2011). Proteolipidic composition of exosomes changes during reticulocyte maturation. *J. Biol. Chem.* **286**, 34426-34439.

Escola, J. M., Kleijmeer, M. J., Stoorvogel, W., Griffith, J. M., Yoshie, O. and Geuze, H. J. (1998). Selective enrichment of tetraspan proteins on the internal vesicles of multivesicular endosomes and on exosomes secreted by human B-lymphocytes. *J. Biol. Chem.* **273**, 20121-20127.

Fevrier, B., Vilette, D., Archer, F., Loew, D., Faigle, W., Vidal, M., Laude, H. and Raposo, G. (2004). Cells release prions in association with exosomes. *Proc. Natl. Acad. Sci. USA* **101**, 9683-9688.

Géminard, C., De Gassart, A., Blanc, L. and Vidal, M. (2004). Degradation of AP2 during reticulocyte maturation enhances binding of hsc70 and Alix to a common site on TFR for sorting into exosomes. *Traffic* **5**, 181-193.

Goujon, C., Jarrosson-Wuillème, L., Bernaud, J., Rigal, D., Darlix, J. L. and Cimarelli, A. (2006). With a little help from a friend: increasing HIV transduction of monocyte-derived dendritic cells with virion-like particles of SIV(MAC). *Gene Ther.* **13**, 991-994.

Gould, S. J. and Raposo, G. (2013). As we wait: coping with an imperfect nomenclature for extracellular vesicles. *J. Extracell. Vesicles* **2**, 20389.

Hanson, P. I. and Cashikar, A. (2012). Multivesicular body morphogenesis. *Annu. Rev. Cell Dev. Biol.* **28**, 337–362.

Harding, C., Heuser, J. and Stahl, P. (1983). Receptor-mediated endocytosis of transferrin and recycling of the transferrin receptor in rat reticulocytes. *J. Cell Biol.* **97**, 329-339.

Henne, W. M., Buchkovich, N. J. and Emr, S. D. (2011). The ESCRT pathway. *Dev. Cell* **21**, 77-91.

Hurley, J. H. (2008). ESCRT complexes and the biogenesis of multivesicular bodies. *Curr. Opin. Cell Biol.* **20**, 4-11.

Hurley, J. H. and Hanson, P. I. (2010). Membrane budding and scission by the ESCRT machinery: it's all in the neck. *Nat. Rev. Mol. Cell Biol.* **11**, 556-566.

Lambert, B., Vandeputte, J., Remacle, S., Bergiers, I., Simonis, N., Twizere, J. C., Vidal, M. and Rezsohazy, R. (2012). Protein interactions of the transcription factor Hoxa1. *BMC Dev. Biol.* **12**, 29.

Landmann, S., Mühlethaler-Mottet, A., Bernasconi, L., Suter, T., Waldburger, J. M., Masternak, K., Arrighi, J. F., Hauser, C., Fontana, A. and Reith, W. (2001). Maturation of dendritic cells is accompanied by rapid transcriptional silencing of class II transactivator (CIITA) expression. *J. Exp. Med.* **194**, 379-392.

Malerød, L., Stuffers, S., Brech, A. and Stenmark, H. (2007). Vps22/EAP30 in ESCRT-II mediates endosomal sorting of growth factor and chemokine receptors destined for lysosomal degradation. *Traffic* **8**, 1617-1629.

Möbius, W., Ohno-Iwashita, Y., van Donselaar, E. G., Oorschot, V. M., Shimada, Y., Fujimoto, T., Heijnen, H. F., Geuze, H. J. and Slot, J. W. (2002). Immunoelectron microscopic localization of cholesterol using biotinylated and non-cytolytic perfringolysin O. *J. Histochem. Cytochem.* **50**, 43-55.

Möbius, W., van Donselaar, E., Ohno-Iwashita, Y., Shimada, Y., Heijnen, H. F., Slot, J. W. and Geuze, H. J. (2003). Recycling compartments and the internal vesicles of multivesicular bodies harbor most of the cholesterol found in the endocytic pathway. *Traffic* **4**, 222-231.

Moffat, J., Grueneberg, D. A., Yang, X., Kim, S. Y., Kloepfer, A. M., Hinkle, G., Piqani, B., Eisenhaure, T. M., Luo, B., Grenier, J. K. et al. (2006). A lentiviral RNAi library for human and mouse genes applied to an arrayed viral high-content screen. *Cell* **124**, 1283-1298.

Ostrowski, M., Carmo, N. B., Krumeich, S., Fanget, I., Raposo, G., Savina, A., Moita, C. F., Schauer, K., Hume, A. N., Freitas, R. P. et al. (2010). Rab27a and Rab27b control different steps of the exosome secretion pathway. *Nat. Cell Biol.* **12**, 19-30; **Suppl.**, 11-13.

Pan, B. T., Teng, K., Wu, C., Adam, M. and Johnstone, R. M. (1985). Electron microscopic evidence for externalization of the transferrin receptor in vesicular form in sheep reticulocytes. *J. Cell Biol.* **101**, 942-948.

Perez-Hernandez, D., Gutiérrez-Vázquez, C., Jorge, I., López-Martín, S., Ursa, A., Sánchez-Madrid, F., Vázquez, J. and Yáñez-Mó, M. (2013). The intracellular interactome of tetraspanin-enriched microdomains reveals their function as sorting machineries toward exosomes. *J. Biol. Chem.* **288**, 11649-11661.

Raiborg, C. and Stenmark, H. (2009). The ESCRT machinery in endosomal sorting of ubiquitylated membrane proteins. *Nature* **458**, 445-452.

Raposo, G. and Stoorvogel, W. (2013). Extracellular vesicles: exosomes, micro-vesicles, and friends. *J. Cell Biol.* **200**, 373-383.

Raposo, G., Nijman, H. W., Stoorvogel, W., Liejendekker, R., Harding, C. V., Melief, C. J. and Geuze, H. J. (1996). B lymphocytes secrete antigen-presenting vesicles. *J. Exp. Med.* **183**, 1161-1172.

Raposo, G., Tenza, D., Murphy, D. M., Berson, J. F. and Marks, M. S. (2001). Distinct protein sorting and localization to premelanosomes, melanosomes, and lysosomes in pigmented melanocytic cells. *J. Cell Biol.* **152**, 809-824.

Razi, M. and Futter, C. E. (2006). Distinct roles for Tsg101 and Hrs in multivesicular body formation and inward vesiculation. *Mol. Biol. Cell* **17**, 3469-3483.

Roxrud, I., Stenmark, H. and Malerød, L. (2010). ESCRT & Co. *Biol. Cell* **102**, 293-318.

Satoh, T. and Manel, N. (2013). Gene transduction in human monocyte-derived dendritic cells using lentiviral vectors. *Methods Mol. Biol.* **960**, 401-409.

Shin, J. S., Ebersold, M., Pypaert, M., Delamarre, L., Hartley, A. and Mellman, I. (2006). Surface expression of MHC class II in dendritic cells is controlled by regulated ubiquitination. *Nature* **444**, 115-118.

Stuffers, S., Sem Wegner, C., Stenmark, H. and Brech, A. (2009). Multivesicular endosome biogenesis in the absence of ESCRTs. *Traffic* **10**, 925-937.

Tamai, K., Tanaka, N., Nakano, T., Kakazu, E., Kondo, Y., Inoue, J., Shiina, M., Fukushima, K., Hoshino, T., Sano, K. et al. (2010). Exosome secretion of dendritic cells is regulated by Hrs, an ESCRT-0 protein. *Biochem. Biophys. Res. Commun.* **399**, 384-390.

Theos, A. C., Truschel, S. T., Tenza, D., Hurbain, I., Harper, D. C., Berson, J. F., Thomas, P. C., Raposo, G. and Marks, M. S. (2006). A lumenal domain-dependent pathway for sorting to intralumenal vesicles of multivesicular endosomes involved in organelle morphogenesis. *Dev. Cell* **10**, 343-354.

Théry, C., Regnault, A., Garin, J., Wolfers, J., Zitvogel, L., Ricciardi-Castagnoli, P., Raposo, G. and Amigorena, S. (1999). Molecular characterization of dendritic cell-derived exosomes. Selective accumulation of the heat shock protein hsc73. *J. Cell Biol.* **147**, 599-610.

Théry, C., Boussac, M., Véron, P., Ricciardi-Castagnoli, P., Raposo, G., Garin, J. and Amigorena, S. (2001). Proteomic analysis of dendritic cell-derived exosomes: a secreted subcellular compartment distinct from apoptotic vesicles. *J. Immunol.* **166**, 7309-7318.

Théry, C., Amigorena, S., Raposo, G. and Clayton, A. (2006). Isolation and characterization of exosomes from cell culture supernatants and biological fluids. *Curr. Protoc. Cell Biol.* **Chapter 3**, Unit 3.22.

Trajkovic, K., Hsu, C., Chiantia, S., Rajendran, L., Wenzel, D., Wieland, F., Schwille, P., Brügger, B. and Simons, M. (2008). Ceramide triggers budding of exosome vesicles into multivesicular endosomes. *Science* **319**, 1244-1247.

van Niel, G., Raposo, G., Candalh, C., Boussac, M., Hershberg, R., Cerf-Bensussan, N. and Heyman, M. (2001). Intestinal epithelial cells secrete exosome-like vesicles. *Gastroenterology* **121**, 337-349.

van Niel, G., Wubbolts, R., Ten Broeke, T., Buschow, S. I., Ossendorp, F. A., Melief, C. J., Raposo, G., van Balkom, B. W. and Stoorvogel, W. (2006). Dendritic cells regulate exposure of MHC class II at their plasma membrane by oligoubiquitination. *Immunity* **25**, 885-894.

van Niel, G., Charrin, S., Simoes, S., Romao, M., Rochin, L., Saftig, P., Marks, M. S., Rubinstein, E. and Raposo, G. (2011). The tetraspanin CD63 regulates ESCRT-independent and -dependent endosomal sorting during melanogenesis. *Dev. Cell* **21**, 708-721.

Viaud, S., Ploix, S., Lapierre, V., Théry, C., Commere, P. H., Tramalloni, D., Gorrichon, K., Virault-Rocroy, P., Tursz, T., Lantz, O. et al. (2011). Updated technology to produce highly immunogenic dendritic cell-derived exosomes of clinical grade: a critical role of interferon-γ. *J. Immunother.* **34**, 65-75.

White, I. J., Bailey, L. M., Aghakhani, M. R., Moss, S. E. and Futter, C. E. (2006). EGF stimulates annexin 1-dependent inward vesiculation in a multivesicular endosome subpopulation. *EMBO J.* **25**, 1-12.

Wollert, T., Wunder, C., Lippincott-Schwartz, J. and Hurley, J. H. (2009). Membrane scission by the ESCRT-III complex. *Nature* **458**, 172-177.

Wubbolts, R., Leckie, R. S., Veenhuizen, P. T., Schwarzmann, G., Möbius, W., Hoernschemeyer, J., Slot, J. W., Geuze, H. J. and Stoorvogel, W. (2003). Proteomic and biochemical analyses of human B cell-derived exosomes. Potential implications for their function and multivesicular body formation. *J. Biol. Chem.* **278**, 10963-10972.

Zitvogel, L., Regnault, A., Lozier, A., Wolfers, J., Flament, C., Tenza, D., Ricciardi-Castagnoli, P., Raposo, G. and Amigorena, S. (1998). Eradication of established murine tumors using a novel cell-free vaccine: dendritic cell-derived exosomes. *Nat. Med.* **4**, 594-600.

Journal of Cell Science